Contribution of the carbon-originated hole trap to slow decays of photoluminescence and photoconductivity in homoepitaxial n-type GaN layers

Masashi Kato[1,3,4*], Takato Asada[1], Takuto Maeda,[1] Kenji Ito[2], Kazuyoshi Tomita[2], Tetsuo Narita[2], Tetsu Kachi[3]

[1]*Department of Electric & Mechanical Engineering, Nagoya Institute of Technology, Nagoya 466-8555, Japan*

[2]*Toyota Central R&D Labs., Inc., Yokomichi41-1, Nagakute 480-1192, Japan*

[3]*Institute of Materials and Systems for Sustainability, Nagoya University, Nagoya 464-8603, Japan*

[4]*Frontier Research institute for Materials Science, Nagoya Institute of Technology, Nagoya 466-8555, Japan*

E-mail: kato.masashi@nitech.ac.jp

Abstract

N-type GaN epitaxial layers grown via metal organic vapor-phase epitaxy typically exhibit a yellow luminescence (YL) band owing to carbon-related deep levels in the photoluminescence spectra. The decay of YL after a pulse excitation involves a long time constant (~0.2 ms at room temperature), whereas microwave photoconductivity decay (μ-PCD) curves show the corresponding component of the time constant. To clarify the origin of the long decay time, the temperature-dependent time constants of YL decay and μ-PCD curves are analyzed using a numerical model based on rate equations for trapping and emission through a deep level. The characteristics of the decays are well reproduced by a recombination model using a hole trap H1 at an energy of E_V +0.88 eV because of the acceptor-like state of carbon on a nitrogen site (C_N) whose electron capture cross section (σ_n) is estimated to be 3×10^{-21} cm^2. The slow decay in μ-PCD signals indicates that the electrons before being captured to H1 traps are free electrons in the conduction band. These findings indicate that the slow recombination process through C_N results in tail currents in the turn-off switching periods of devices.

Introduction

GaN possesses superior physical properties required for power devices compared with Si owing to its wide bandgap and high breakdown electric field. In particular, vertical device structures using GaN homoepitaxial layers on freestanding GaN substrates are promising for low-loss and high-voltage operations.[1-3] An important factor in vertical structures is the crystalline quality of homoepitaxial n-type layers, which serve as electron drift layers for blocking high voltages. However, deep levels formed via point defects in GaN homoepitaxial layers have not been fully elucidated, although carrier trapping into

deep levels can affect the switching performance in devices. Therefore, it is essential to identify deep levels that affect device performances. N-type homoepitaxial GaN drift layers are generally grown via metal organic vapor-phase epitaxy (MOVPE), which affords a precise control of impurity doping and thickness. However, during MOVPE growth, impurities such as carbon, hydrogen, and iron atoms are unintentionally incorporated into the epitaxial layers, resulting in carrier trapping via deep levels.[4-8]

Various characterization results for deep levels in GaN epitaxial layers have been obtained using deep level transient spectroscopy (DLTS), photoluminescence (PL), time-resolved photoluminescence (TR-PL), and microwave photoconductivity decay (μ-PCD).[9-22] Among these characterization techniques, TR-PL and μ-PCD enable the evaluation of time-dependent carrier recombination and are highly sensitive to deep levels. An n-type GaN layer typically shows slow decay components in TR-PL and μ-PCD decay curves, whereas some of the deep levels in GaN are accompanied with broad luminescence bands represented by yellow luminescence (YL).[4-6] Hence, the relation between the YL band and slow carrier recombination has been discussed.[23] Many studies have been conducted to elucidate the physical origin and mechanism of YL; currently, the most plausible origin of YL is carrier recombination through a deep level generated by carbon on a nitrogen site (C_N).[24-29] The slow transition through the C_N level is expected to result in persistent photoconductivity; however, the relation between conductivity and the YL band is not fully elucidated. If C_N causes a low conductivity, subsequently it can degrade the switching performance in a device composed of an MOVPE-grown n-type GaN drift layer. In this study, to understand the effect of C_N, we focused on the temperature dependence of TR-PL and μ-PCD decay curves. Subsequently, we analyzed the results using a numerical model with the rate equations for trapping and emission through a deep level to identify the effects of the C_N level on TR-PL and μ-PCD decay curves.

Experiments

We used two samples with n-type homoepitaxial GaN layers grown via MOVPE on freestanding GaN substrates. The substrate for one of the samples, labeled S1, was n-type GaN doped with Si, whereas the substrate for the other sample, labeled S2, was a semi-insulating GaN doped with Fe. Although semi-insulating substrates are not typically used for power device applications, they enable the extraction of only the conductivity of the upper epitaxial layer in μ-PCD signals, owing to their low conductivity at equilibrium. During MOVPE growth in this study, Si was intentionally doped, but C was unintentionally doped. Subsequently, the Si and C concentrations and uniformities were confirmed via secondary ion mass spectrometry (SIMS). Detailed information regarding the samples is summarized in Table I. Although the epilayer thicknesses were different between S1 and S2, both the thicknesses were enough to characterize bulk characteristics in the epilayers considering penetration depth of the light and carrier diffusion length. The PL spectra from the samples were detected using a multichannel spectrometer. In TR-PL measurements, we employed a Si photodiode or a photomultiplier as the detector. To measure the YL decay, a long pass filter (LPF) with a cutoff wavelength of 461 nm (2.69 eV) was inserted in front of the detector. In μ-PCD measurements, we employed 10 GHz microwaves as a probe and detected the reflection of the microwaves from the samples. The μ-PCD signals from S2 were obtained, whereas those from S1 did not exhibit a clear decay curve owing to the significant noise from the conductive substrate. TR-PL measurements were performed at 300 to 623 K using a hot plate, whereas μ-PCD measurements were performed up to 523 K owing to the limitations of the optical system. For all the measurements, an excitation by a yttrium aluminum garnet laser of 266 or 355 nm was employed, and, for GaN, their penetration depths were less than 150 nm.[30] A pulse width and a repetition rate of the lasers were 1 ns and 100 Hz, respectively. The injected photon density was set to ~10^{14} cm^{-2}.

Table I. Summary of samples.

Name	S1	S2
Thickness of top layer	10 μm	2 μm
Si concentration of top layer	5×10^{16} cm^{-3}	4×10^{16} cm^{-3}
C concentration of top layer	3×10^{15} cm^{-3}	8×10^{15} cm^{-3}
Substrate	Si-doped n-type GaN	Fe-doped semi-insulating GaN

Results

The PL spectra for S1 and S2 at room temperature are shown in Fig. 1, where the PL intensities were normalized by the intensities of the near-band-edge emission. For both samples, the PL spectra comprised the near band edge at and YL below 2.7 eV. The relative YL intensity of S1 was higher than that of S2, and the YL spectra shapes of S1 and S2 differed.

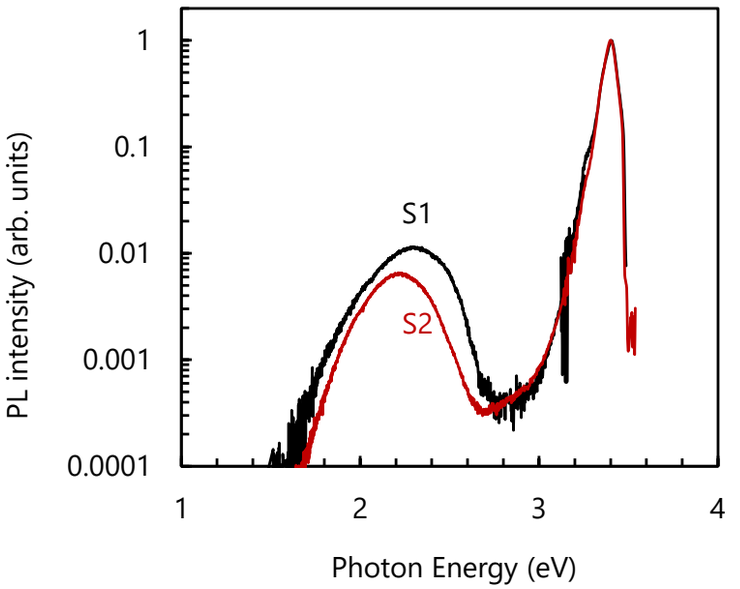

Fig. 1. PL spectra for samples at room temperature with normalization by near band edge luminescence intensity.

Figure 2 shows the TR-PL decay curves for S1 and S2 at room temperature in double logarithmic plots, in which each exponential decay component appeared as a shoulder in the curves. The faster component was observed in S1, and it indicated a time constants of 1–10 μs. Meanwhile, the slower components were observed in both samples, and their time constants were 200–400 μs. The similar decay trends for the cases with and without an LPF indicate that the decay involved wavelengths longer than 461 nm, which corresponded to a YL photon energy of less than 2.69 eV, as shown in Fig. 1. The faster components in the decay from S1 contributed to the relatively high YL intensity as shown in Fig. 1.

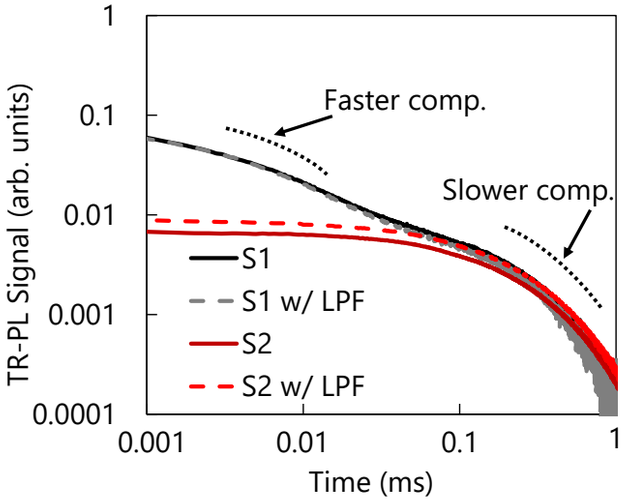

Fig. 2. TR-PL decay curves for S1 and S2 at room temperature without filter (full spectrum) and with 461 nm LPF in double-logarithmic plot.

Figure 3 shows the temperature dependence of the TR-PL decay curves without an LPF for S1. The slower component exhibited similar time constants of 200–260 μs below 473 K, and the time constant

decreased as the temperature increased beyond 473 K. This temperature dependence is consistent with the previously reported temperature dependence of YL intensities and decay time constants.[9,29]

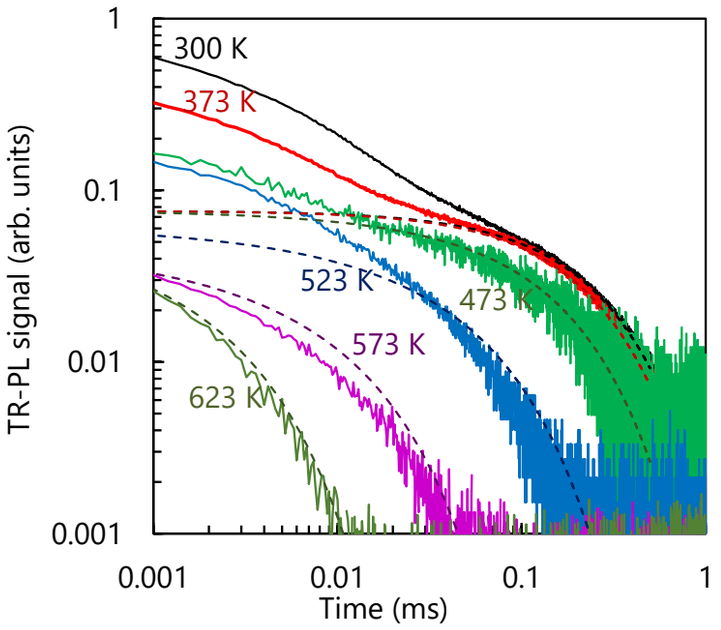

Fig. 3. Temperature dependence of TR-PL decay curves without LPF for S1. Solid lines represent experimental results; dashed lines represent results calculated using parameters listed in Table II, with $N_R = 1 \times 10^{16}$ cm^{-3} and $\sigma_n^T = 1 \times 10^{-21}$ cm^2.

Figure 4 shows the temperature dependence of the TR-PL and μ-PCD decay curves for S2. Similar to the case of S1, the time constants of the TR-PL decay curves decreased as the temperature increased beyond 473 K; similarly, the time constants of the μ-PCD decay curves decreased with increasing temperature.

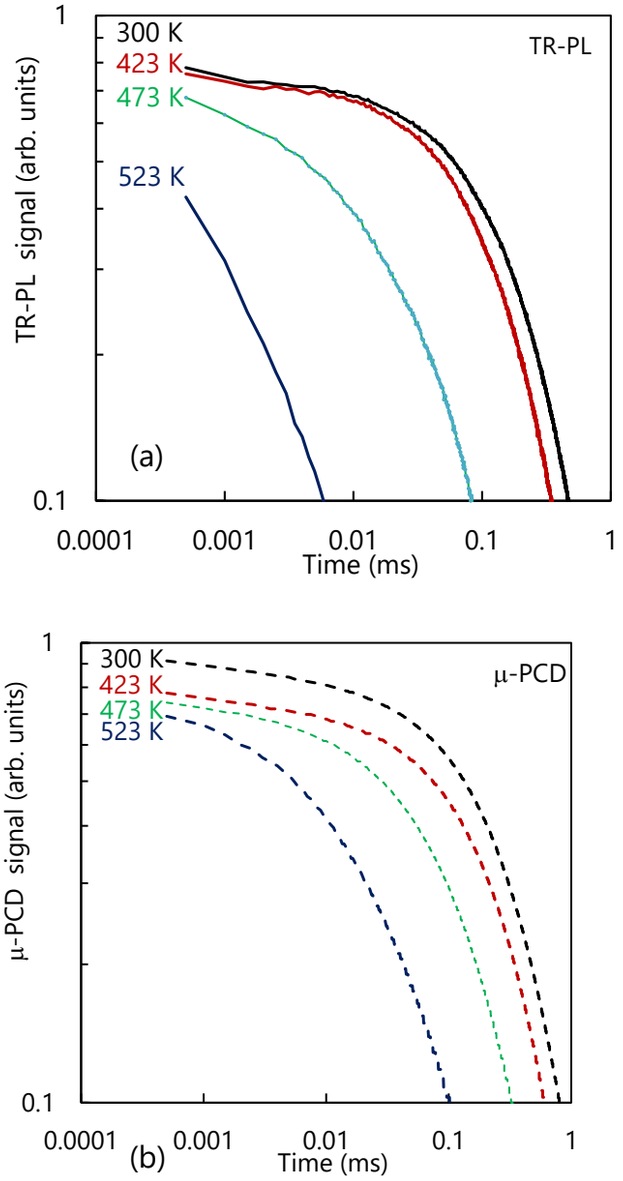

Fig. 4. Temperature dependence of (a) TR-PL (without LPF), and (b) μ-PCD decay curves for S2.

Numerical modeling

To explain the temperature dependence of the time constants in the TR-PL and μ-PCD decay curves, we performed calculations pertaining to the decay curves based on the rate equations of carrier trapping

and emission.[31-33] The slow decay of excited carriers is generally caused by the trapping of excited minority carriers at deep levels, as schematically shown in Fig. 5, which depicts a band diagram with deep levels behaving as a hole trap (H1) and a recombination channel. The recombination channel represents fast recombination, including radiative and nonradiative recombination, whose maximum lifetime is expected to be 1 ns even in high-quality GaN layers.[13] Therefore, the recombination lifetime is extremely short and cannot be observed in the present time scale of TR-PL and μ-PCD analyses. After carrier excitation, the initial free holes immediately disappeared from the valence band owing to recombination through the recombination channels and trapping into the hole traps. However, after the free holes disappeared, excess free electrons remained in the conduction band. At low temperatures, the excess free electrons recombined with trapped holes in deep levels. If the electron capture cross-section at the hole trap is extremely small, then the time constant of the transition will be long. With increasing temperature, the holes were emitted from the traps to the valence band and subsequently recombined with excess free electrons through the recombination channel. Therefore, an increase in the temperature resulted in a decrease in the time constant of the slow decay.

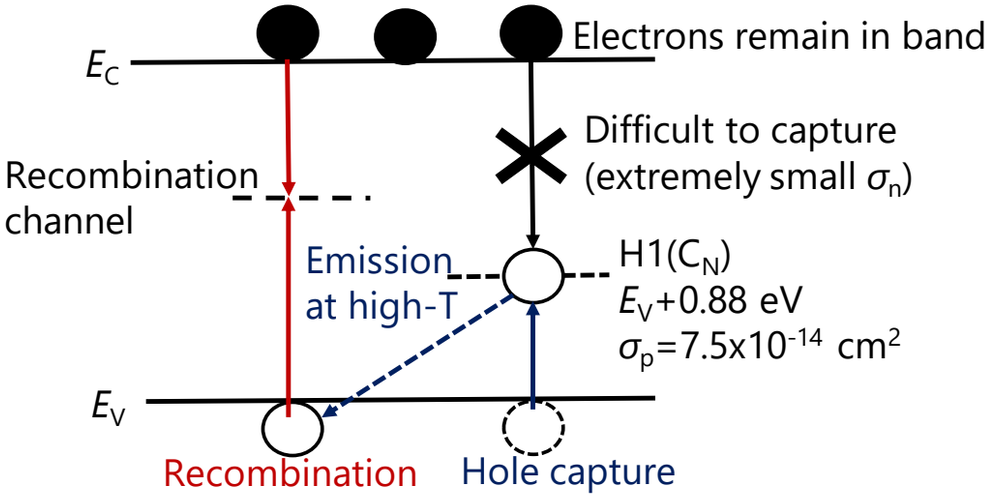

Fig. 5. Schematic illustration of analytical model based on energy band representation. E_C and E_V indicate edges of conduction and valence bands, respectively.

Using this model, we calculated the temporal change in the concentrations of free electrons n and free holes p using the following equations:[31]

$$\frac{\mathrm{d}n}{\mathrm{d}t} = -\sigma_n^{\mathrm{T}} v_{\mathrm{th}} n(N_{\mathrm{T}} - n_{\mathrm{T}}) + e_{\mathrm{n}}^{\mathrm{T}} n_{\mathrm{T}} - \sigma_{\mathrm{n}}^{\mathrm{R}} v_{th} n(N_R - n_R) + e_n^R n_R \qquad (1),$$

and

$$\frac{\mathrm{d}p}{\mathrm{d}t} = -\sigma_{\mathrm{p}}^{\mathrm{T}} v_{\mathrm{th}} p n_{\mathrm{T}} + e_{\mathrm{p}}^{\mathrm{T}}(N_{\mathrm{T}} - n_{\mathrm{T}}) - \sigma_{\mathrm{p}}^{\mathrm{R}} v_{\mathrm{th}} p n_{\mathrm{R}} + e_{\mathrm{p}}^{\mathrm{R}}(N_{\mathrm{R}} - n_{\mathrm{R}}) \qquad (2),$$

where $\sigma_{\mathrm{n}}^{\mathrm{T}}$ ($\sigma_{\mathrm{p}}^{\mathrm{T}}$) is the capture cross-section of the trap for electrons (holes), v_{th} the thermal velocity of the carriers, N_{T} (N_{R}) the concentration of the trap (the recombination center), n_{T} (n_{R}) the electron concentration at the trap (the recombination center), and $e_{\mathrm{n}}^{\mathrm{T}}$ ($e_{\mathrm{p}}^{\mathrm{T}}$) the emission coefficient for the electrons (holes) in the trap. The superscript "R" of σ and e indicates the values for the recombination center. The relationship between $e_{\mathrm{n}}^{\mathrm{T}}$ and $\sigma_{\mathrm{n}}^{\mathrm{T}}$ is expressed as

$$e_{\mathrm{n}}^{\mathrm{T}} = \sigma_{\mathrm{n}}^{\mathrm{T}} v_{\mathrm{th}} N_{\mathrm{C}} \exp\left(\frac{-(E_{\mathrm{c}} - E_{\mathrm{T}})}{kT}\right) \qquad (3),$$

where Nc is the effective density of states for the conduction band. A similar relationship holds between $e_{\mathrm{p}}^{\mathrm{T}}$ and $\sigma_{\mathrm{p}}^{\mathrm{T}}$, and also for the recombination center. To calculate Nc and the effective density of states for the valence band Nv, which is employed in the relationship between $e_{\mathrm{p}}^{\mathrm{T}}$ and $\sigma_{\mathrm{p}}^{\mathrm{T}}$, we adopted the effective masses of electrons and holes of $0.2m_0$ and $0.9m_0$, respectively,[34,35] where m_0 is the rest electron mass. Similarly, the rate equations for the trap and recombination center are

$$\frac{\mathrm{d}n_{\mathrm{T}}}{\mathrm{d}t} = \sigma_{\mathrm{n}}^{\mathrm{T}} v_{\mathrm{th}} n(N_{\mathrm{T}} - n_{\mathrm{T}}) - e_{\mathrm{n}}^{\mathrm{T}} n_{\mathrm{T}} - \sigma_{\mathrm{n}}^{\mathrm{T}} v_{\mathrm{th}} p n_{\mathrm{T}} + e_{\mathrm{n}}^{\mathrm{T}}(N_{\mathrm{T}} - n_{\mathrm{T}}) \quad (4),$$

and

$$\frac{dn_R}{dt} = \sigma_n^R v_{th} n(N_R - n_R) - e_n^R n_R - \sigma_n^R v_{th} p n_R + e_n^R (N_R - n_R) \quad (5),$$

respectively. The TR-PL decay curves for the band edge emission can be obtained by calculating n and p as the band-to-band PL intensity $I_{PL} \propto n \cdot p$. Next, we focus on the slow decay component in TR-PL, which corresponds to recombination at the trap. Therefore, to reproduce the slow decay components, we calculated the intensity of YL $I_{YL} \propto n \cdot (N_T - n_T)$. Furthermore, a μ-PCD signal represents conductivity via all free carriers. Therefore, we reproduced the signals based on $\mu_n \cdot n + \mu_p \cdot p$, where μ_n and μ_p represent the electron and hole mobilities, respectively.

The initial excess carrier concentration was set to 1×10^{18} cm^{-3} considering the penetration depth and injected photon density of the lasers in the experiments. The recombination center does not signify a specific level but includes all radiative and nonradiative components. Meanwhile, the virtual energy level E_R and capture cross-section for the electrons and holes were assumed to be E_V + 1.7 eV $\sigma_n^R = \sigma_p^R = 10^{-15}$ cm^2. The concentration of the recombination center N_R was a variable parameter. We assigned H1, which is associated with the acceptor level of C_N, as the hole trap.[17] The parameters of H1 were assumed to be $E_T = E_V$ + 0.88 eV and $\sigma_p^T = 7.5 \times 10^{-14}$ cm^2, which were estimated via DLTS measurements for p-type GaN.[18] The trap concentration N_T was 3 or 8 × 10^{15} cm^{-3}, which corresponded to the carbon concentration in the samples, whereas σ_n^T was a variable parameter. The parameters used are summarized in Table II.

Table II. Parameters used for calculation of rate equations.

	Hole trap (H1)	Recombination center
Energy level (E_T)	E_V + 0.88 eV	E_V + 1.7 eV
Electron capture cross-section (σ_n)	Variable	10^{-15} cm^2
Hole capture cross section (σ_p)	7.5×10^{-14} cm^2	10^{-15} cm^2
Concentration	3 or 8 × 10^{15} cm^{-3} (= C concentration)	Variable

A comparison of the experimental and calculated time constants is shown in Fig. 6. For S1, the cutoff temperature, above which the time constant decreased significantly, depended on N_R. The best fit with the experiment was obtained at $N_R = 1 \times 10^{16}$ cm^{-3}. Meanwhile, the time constants below ~450 K depended on σ_n^T, and the experimental values were reproduced for the case where σ_n^T was 3×10^{-21} cm^2. The dependence of the time constants on σ_n^T indicated that the time constant at low temperatures was limited by the electron capture process from the conduction band to the hole trap. The calculated decay curves based on the fitted parameters are shown in Fig. 3. For S2, we reproduced the experimental time constants from the TR-PL and μ-PCD decay curves, as shown in Fig. 7. For both the TR-PL and μ-PCD results, $\sigma_n^T = 3 \times 10^{-21}$ cm^2 showed the best fitting, as in the case of S1. Meanwhile, the best N_R was 1×10^{17} cm^{-3}, which was significantly high compared with that of S1.

The estimated σ_n^T of 3×10^{-21} cm^2 was similar to the reported values of $\sigma_n^T = 1.4 \times 10^{-22}$ or 7×10^{-20} cm^2 of H1.[21,22] Considering the consistency of the TR-PL and μ-PCD results for S2, the YL and slow photoconductivity suggested the same origin and hole trap H1; hence, H1 will significantly affect the tail current in the turn-off switching periods of power devices. Meanwhile, a high N_R was estimated from S2 compared with S1. It has been reported that the Fe in the substrates was incorporated into epilayers at a significant concentration, and,[36] in S2, Fe with ~10^{15} cm^{-3} was confirmed by SIMS. Fe served as a nonradiative recombination center in GaN with large σ_n and σ_p.[37-39] Therefore, the origin of the high N_R for S2 was likely the incorporation of Fe in the epilayer.

The observed slow decay component will appear in any GaN device after hole injection when carbon is present in the n-type GaN. In bipolar devices such as p–n diodes and bipolar junction transistors, hole injection is unavoidable owing to the nature of device operation. Even in unipolar devices, when we employ body diodes of metal–oxide–semiconductor field effect transistors (MOSFETs) to conduct current in the turn-off state, holes are injected into an n-type drift layer.[40] The injected holes gradually recombine

with electrons, inducing a tail current. The slow decay of the tail current contributes to switching losses and limits the operation frequency of the devices. To reduce the effects of the slow decay component, we must grow a drift layer with a low carbon concentration or adopt device structures with suppressed hole injections, such as Schottky barrier diodes integrated with MOSFETs, as reported in SiC.[41] Even though the defect types caused by hole injection differ between GaN and SiC (in the case of SiC, stacking faults are caused by hole injection[42]), hole injection control is important for devices based on both materials.

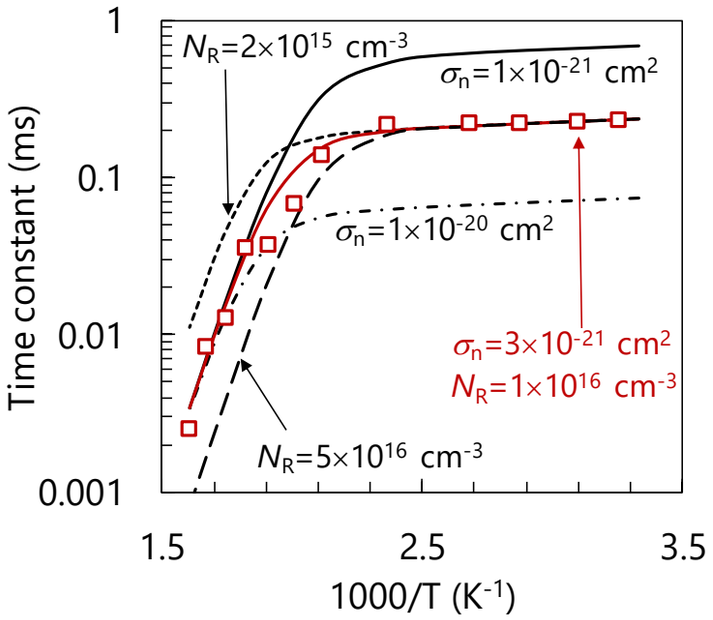

Fig. 6. Temperature dependence of time constants of slower component in TR-PL decay curves for S1. Symbols and lines indicate experimental and calculated results, respectively. Solid red line corresponds to calculation using $N_R = 1 \times 10^{16}$ cm^{-3} and $\sigma_n^T = 3 \times 10^{-21}$ cm^2 for hole trap, whereas others are calculated using different N_R and σ_n^T.

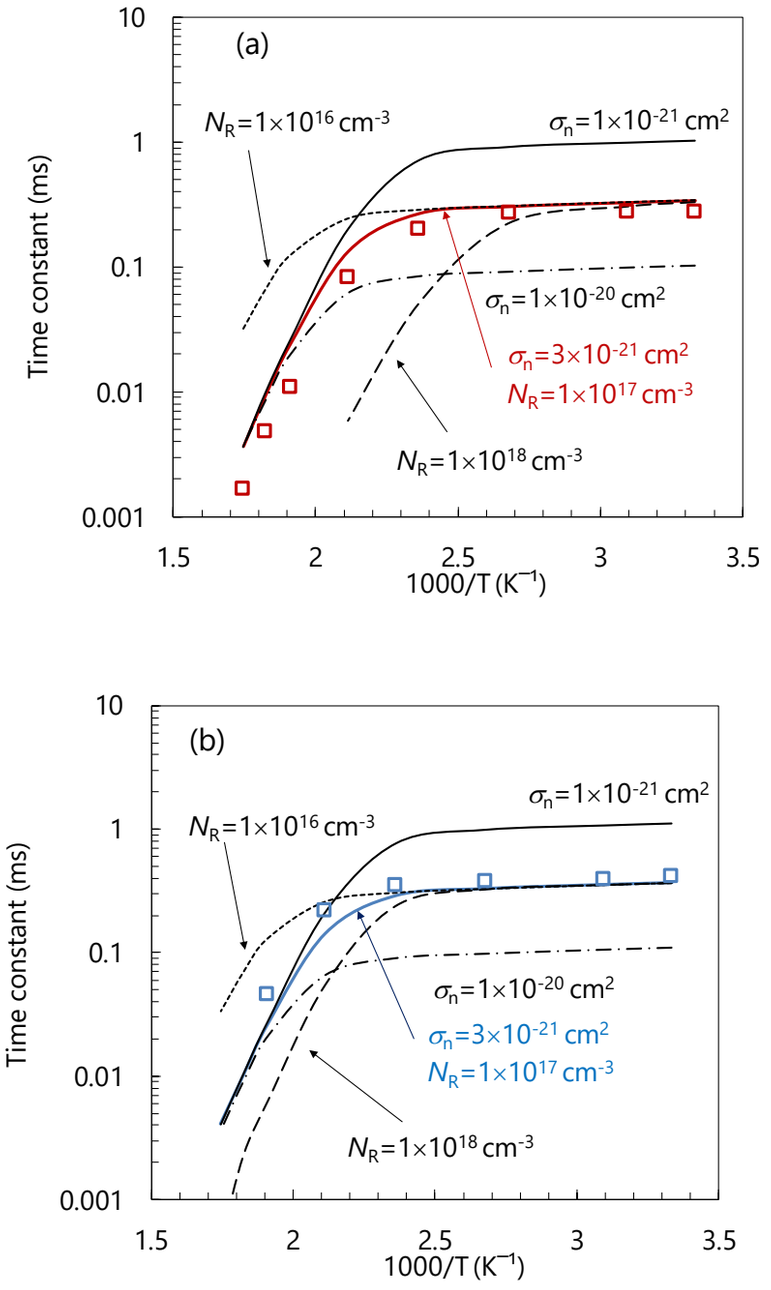

Fig. 7. Temperature dependence of time constants of slower component for S2 in (a) TR-PL, and (b) μ-PCD decay curves. Symbols and lines represent experimental and calculated results, respectively. Solid colored lines correspond to calculation using N_R = 1 × 10^{17} cm^{-3} and σ_n^T = 3 × 10^{-21} cm^2 for hole trap, whereas others are calculated using different N_R and σ_n^T.

Conclusions

We performed TR-PL and μ-PCD measurements at various temperatures on n-type GaN homoepilayers. The slow components of the TR-PL decay curves exhibited a wavelength YL region, and their time constants were correlated to the slow component of μ-PCD. We numerically reproduced the time constants of the slow component in the YL and μ-PCD decay curves based on the model using trapping and emission through the hole trap H1 (the acceptor level of C_N). The σ_n value for H1 was 3×10^{-21} cm^2, and such a small σ_n caused slow decays of YL and μ-PCD signals. The model implied a difference in the concentrations of nonradiative recombination centers among the samples. The μ-PCD signals reflected a conductivity change after the minority carrier injection; hence, H1 will induce a tail current in the turn-off switching periods of power devices. Therefore, the control of carbon concentration is important when fabricating power devices with minority carrier injection.

Acknowledgements

This work was supported by MEXT "Research and development of next-generation semiconductor to realize energy-saving society" Program under Grant No. JPJ005357.

Data Availability

The data that support the findings of this study are available from the corresponding author upon reasonable request.

REFERENCES

[1] T. Oka, Jpn. J. Appl. Phys. 58, SB0805 (2019).

[2] I.C. Kizilyalli, P. Bui-Quang, D. Disney, H. Bhatia, and O. Aktas, Microelectron. Reliab. 55, 1654 (2015).

[3] H. Ohta, N. Kaneda, F. Horikiri, Y. Narita, T. Yoshida, T. Mishima, and T. Nakamura, IEEE Electron Device Lett. 36, 1180 (2015).

[4] I.C. Kizilyalli, A.P. Edwards, O. Aktas, T. Prunty, and D. Bour, IEEE Trans. Electron Devices 62, 414 (2015).

[5] T. Tanaka, N. Kaneda, T. Mishima, Y. Kihara, T. Aoki, and K. Shiojima, Jpn. J. Appl. Phys. 54, (2015).

[6] G. Piao, K. Ikenaga, Y. Yano, H. Tokunaga, A. Mishima, Y. Ban, T. Tabuchi, and K. Matsumoto, J. Cryst. Growth, 456, 137 (2016).

[7] T. Narita, M. Horita, K. Tomita, T. Kachi, and J. Suda, Jpn. J. Appl. Phys. 59, 105505 (2020).

[8] T. Narita, K. Tomita, K. Kataoka, Y. Tokuda, T. Kogiso, H. Yoshida, N. Ikarashi, K. Iwata, M. Nagao, N. Sawada, M. Horita, J. Suda, and T. Kachi, Jpn. J. Appl. Phys. 59, SA0804 (2020).

[9] M. A. Reshchikov, and H. Morkoç, J. Appl. Phys. 97, 061301 (2005).

[10] D. O. Demchenko, I. C. Diallo, and M. A. Reshchikov, Phys. Rev. Lett. 110, 087404 (2013).

[11] M. A. Reshchikov, D. O. Demchenko,and A. Usikov, Pys. Rev. B 90, 235203 (2014).

[12] S. Juršenas, S. Miasojedovas, A. Žukauskas, B. Lucznik, I. Grzegory, and T. Suski, Appl. Phys. Lett. 89, 172119 (2006).

[13] S.F. Chichibu, K. Hazu, Y. Ishikawa, M. Tashiro, H. Namita, S. Nagao, K. Fujito, and a. Uedono, J. Appl. Phys. 111, 103518 (2012).

[14] W. Grieshaber, E. F. Schubert, I. D. Goepfert, R. F. Karlicek, M. J. Schurman, and C. Tran, J. Appl. Phys. 80, 4615 (1996).

[15] M. A. Reshchikov, J. Appl. Phys. 115, 103503 (2014).

[16] M. A. Reshchikov , N. M. Albarakati, M. Monavarian, V. Avrutin, and H. Morkoç, J. Appl. Phys. 123, 161520 (2018).

[17] Y. Tokuda, ECS Trans. 75, 39 (2016).

[18] T. Narita, Y. Tokuda, T. Kogiso, K. Tomita, and T. Kachi, J. Appl. Phys. 123, 161405 (2018).

[19] M. Kato, K. Mikamo, M. Ichimura, M. Kanechika, O. Ishiguro, and T. Kachi, J. Appl. Phys. 103, 093701 (2008).

[20] H. Watanabe, M. Kato, M. Ichimura, E. Arai, M. Kanechika, O. Ishiguro, and T. Kachi, Jpn. J. Appl. Phys. 46, 35 (2007).

[21] A.Y. Polyakov, N.B. Smirnov, E.B. Yakimov, S.A. Tarelkin, A. V. Turutin, I. V. Shemerov, S.J. Pearton, K. Bin Bae, and I.H. Lee, J. Alloys Compd. 686, 1044 (2016).

[22] K. Kanegae, M. Horita, T. Kimoto, and J. Suda, Appl. Phys. Express 11, 071002 (2018).

[23] S. J. Chung, O. H. Cha, Y. S. Kim, C.-H. Hong, H. J. Lee, M. S. Jeong, J. O. White, and E.-K. Suh, J. Appl. Phys. 89, 5454 (2001)

[24] J. Lyons, A. Janotti, and C. G. Van de Walle, Phys. Rev. B 89, 035204 (2014).

[25] J. Lyons, A. Janotti, and C. G. Van De Walle, Appl. Phys. Lett. 97, 152108 (2010).

[26] M. Julkarnain, N. Kamata T. Fukuda, Y. Arakawa. Optical Mater, 60, 481 (2016).

[27] M. Matys and B. Adamowicz, J. Appl. Phys. 121, 065104 (2017).

[28] S. G. Christenson, W. Xie, Y. Y. Sun, S. B. Zhangb , J. Appl. Phys. 118, 135708 (2015).

[29] A. Reshchikov, M. Vorobiov, D.O. Demchenko, Ozgur, H. Morkoç, A. Lesnik, M.P. Hoffmann, F. Hörich, A. Dadgar, and A. Strittmatter, Phys. Rev. B 98, 125207 (2018).

[30] J. F. Muth, J. H. Lee, I. K. Shmagin, R. M. Kolbas, H. C. Casey, Jr., B. P. Keller, U. K. Mishra, and S. P. DenBaars, Appl. Phys. Lett. 71, 2572 (1997).

[31] M. Ichimura, Solid-State Electron. 50, 1761 (2006).

[32] M. Kato, M. Kawai, T. Mori, M. Ichimura, S. Sumie, and H. Hashizume, Jpn. J. Appl. Phys. 46, 5057 (2007).

[33] T. Okuda, H. Miyake, T. Kimoto, and J. Suda, Jpn. J. Appl. Phys. 52, 010202 (2013).

[34] T. Maeda, T. Narita, M. Kanechika, T. Uesugi, T. Kachi, T. Kimoto, M. Horita, and J. Suda, Appl. Phys. Lett. 112, (2018).

[35] Z. Zhang, A. R. Arehart, E. C. H. Kyle, J. Chen, E. X. Zhang, D. M. Fleetwood, R. D. Schrimpf, J. S. Speck, and S. A. Ringel, Appl. Phys. Lett. 106, 022104 (2015).

[36] T. Ishiguro, A. Yamada, J. Kotani, N. Nakamura, T. Kikkawa, K. Watanabe, and K. Imanishi, Jpn. J. Appl. Phys. 52, 162107 (2013).

[37] D. Wickramaratne, J.X. Shen, C.E. Dreyer, M. Engel, M. Marsman, G. Kresse, S. Marcinkevičius, A. Alkauskas, and C.G. Van de Walle, Appl. Phys. Lett. 109, 08JB17 (2016).

[38] T.K. Uždavinys, S. Marcinkevičius, J.H. Leach, K.R. Evans, and D.C. Look, J. Appl. Phys. 119, 215706 (2016).

[39] T. Aggerstam, A. Pinos, S. Marcinkevičius, M. Linnarsson, and S. Lourdudoss, J. Electron. Mater. 36, 1621 (2007).

[40] S. Jahdi, O. Alatise, R. Bonyadi, P. Alexakis, C. A. Fisher, J. A. O. Gonzalez, L. Ran, P. Mawby IEEE Trans. Power Electron. 30, 2383 (2015).

[41] Y. Kobayashi, H. Ishimori, A. Kinoshita, T. Kojima, M. Takei, H. Kimura, and S. Harada, Jpn. J. Appl. Phys. 56, 04CR08 (2017).

[42] M. Skowronski and S. Ha, J. Appl. Phys. 99, 011101 (2006).

AIP Publishing
Journal of Applied Physics
ACCEPTED MANUSCRIPT

PLEASE CITE THIS ARTICLE AS DOI: 10.1063/5.0041287

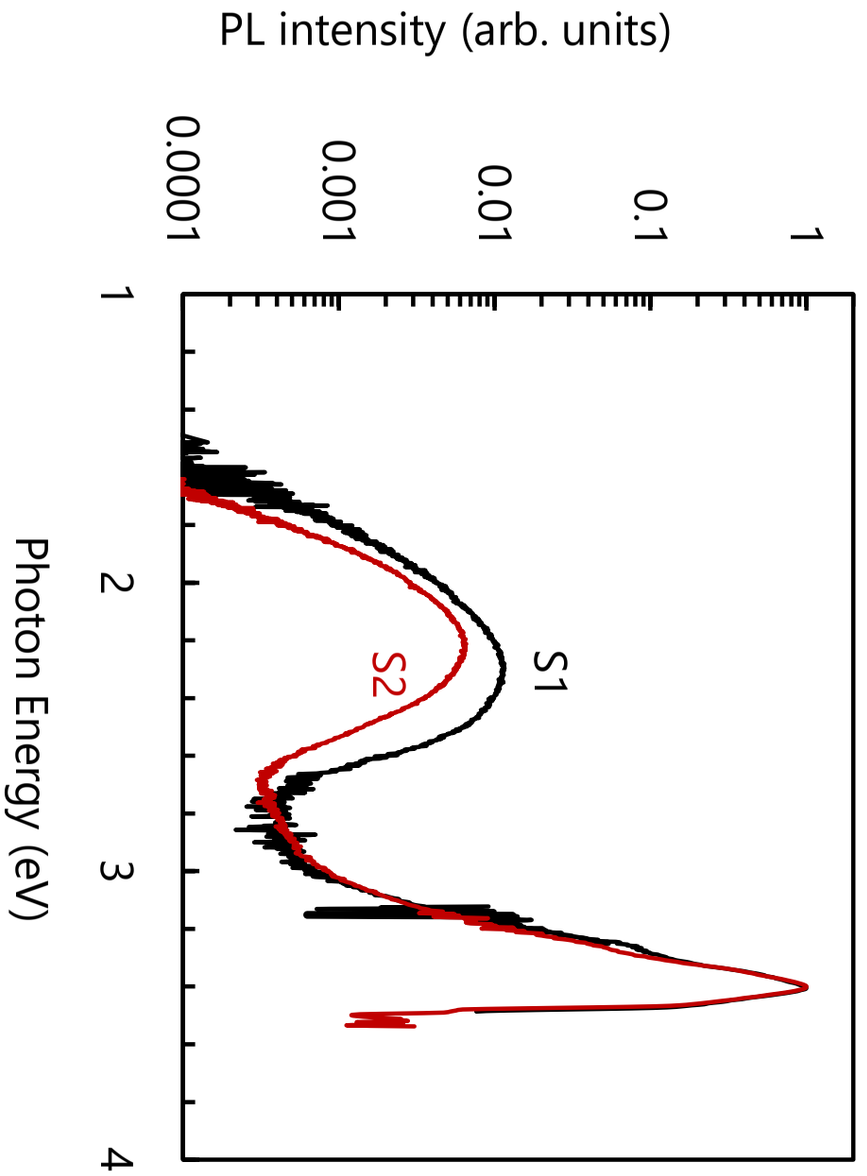

AIP Publishing

Journal of Applied Physics

ACCEPTED MANUSCRIPT

This is the author's peer reviewed, accepted manuscript. However, the online version of record will be different from this version once it has been copyedited and typeset.
PLEASE CITE THIS ARTICLE AS DOI: 10.1063/5.0041287

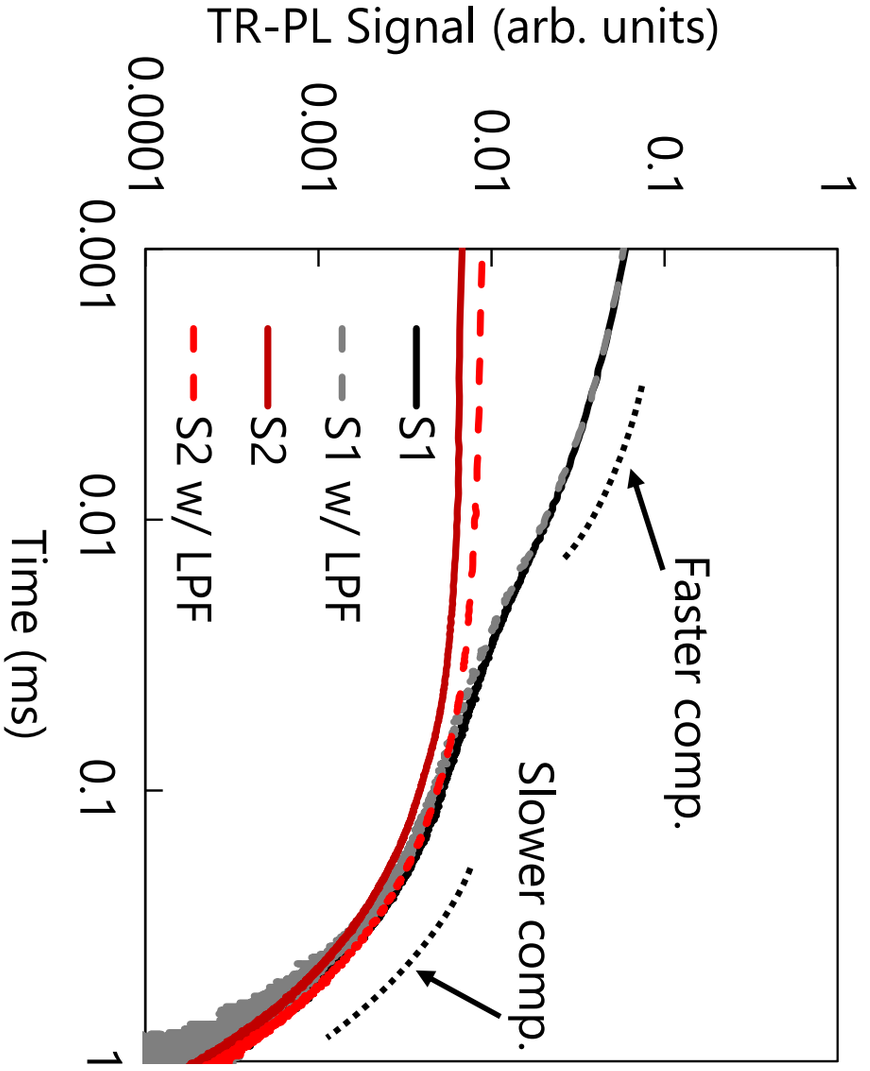

AIP Publishing

Journal of Applied Physics

ACCEPTED MANUSCRIPT

This is the author's peer reviewed, accepted manuscript. However, the online version of record will be different from this version once it has been copyedited and typeset.
PLEASE CITE THIS ARTICLE AS DOI: 10.1063/5.0041287

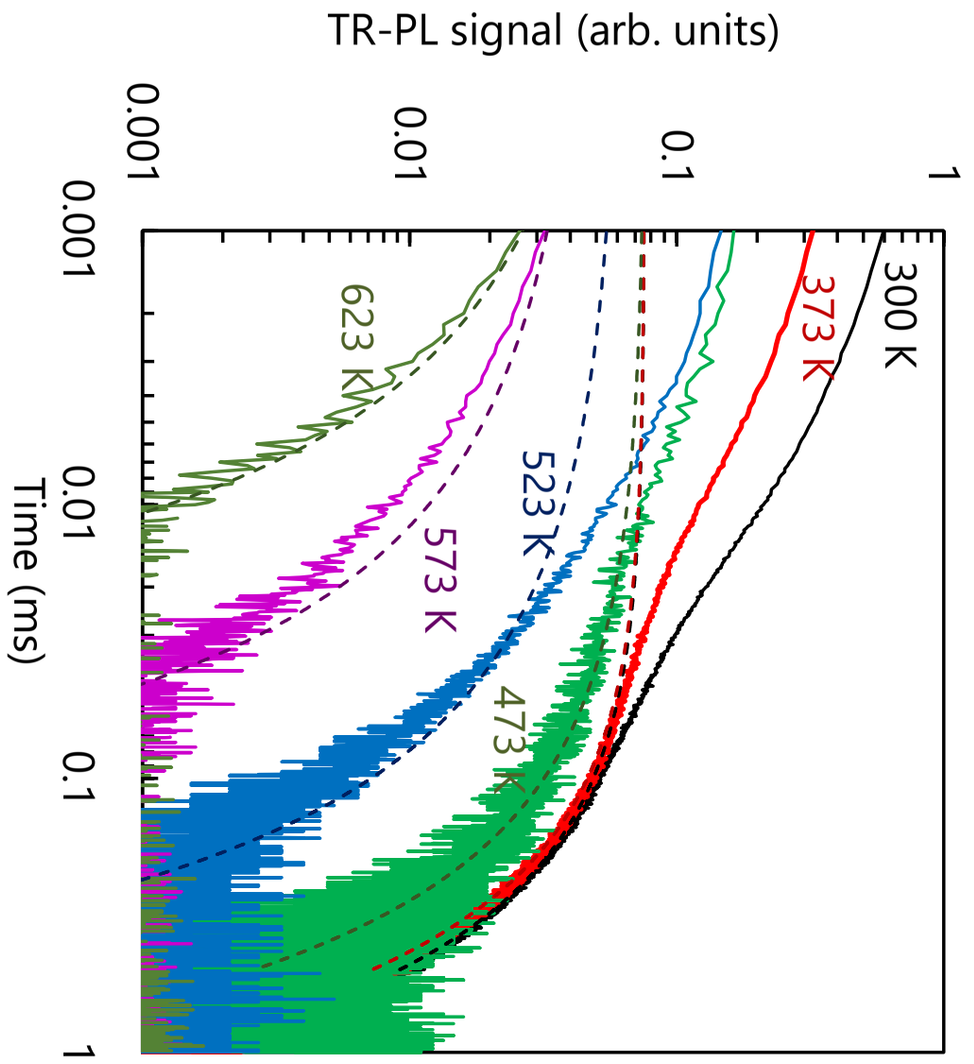

AIP Publishing

Journal of Applied Physics

ACCEPTED MANUSCRIPT

This is the author's peer reviewed, accepted manuscript. However, the online version of record will be different from this version once it has been copyedited and typeset.
PLEASE CITE THIS ARTICLE AS DOI: 10.1063/5.0041287

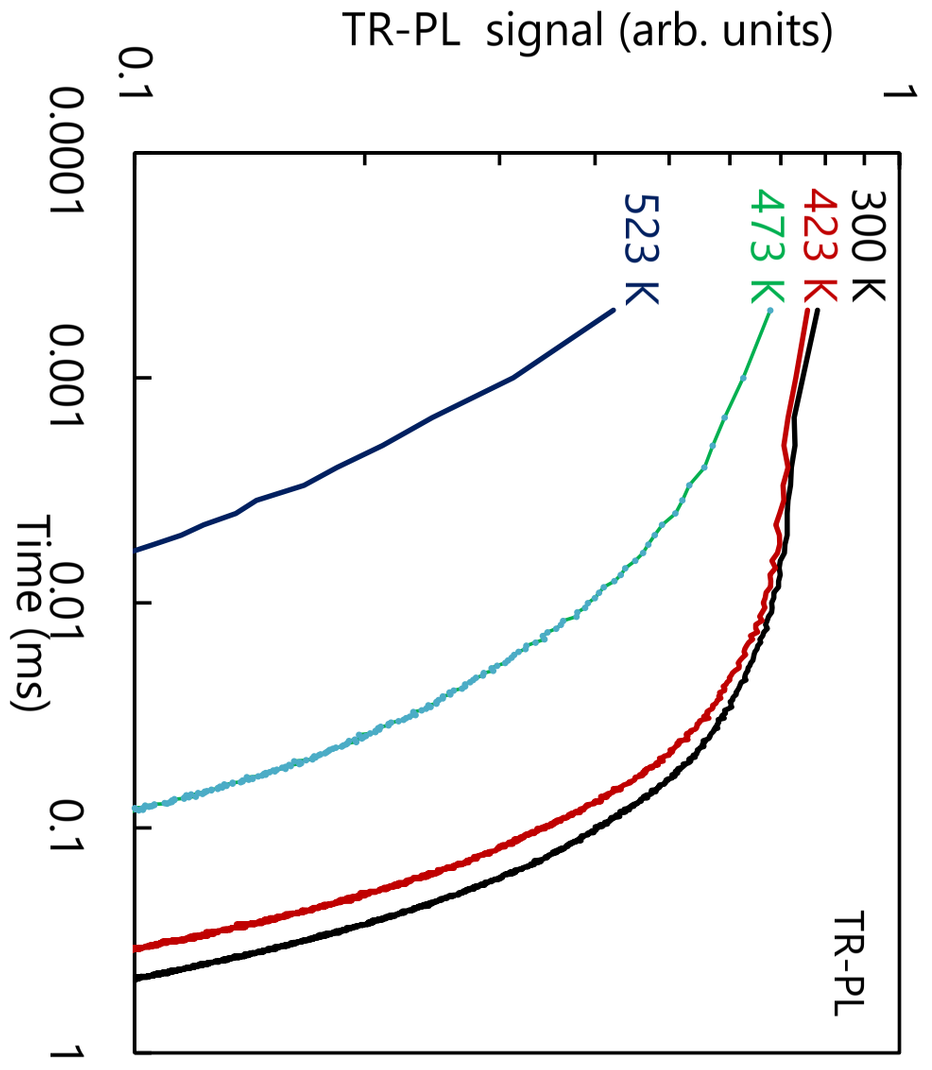

AIP Publishing

Journal of Applied Physics

ACCEPTED MANUSCRIPT

This is the author's peer reviewed, accepted manuscript. However, the online version of record will be different from this version once it has been copyedited and typeset.
PLEASE CITE THIS ARTICLE AS DOI: 10.1063/5.0041287

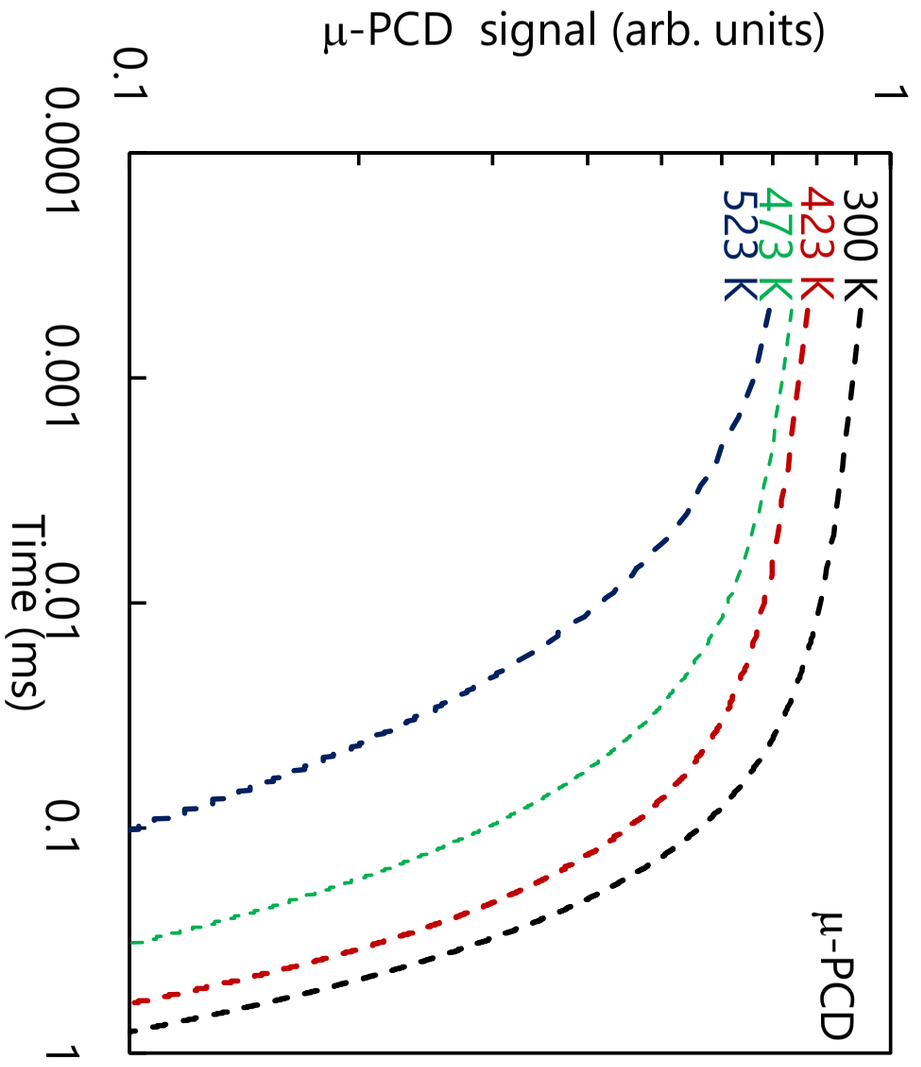

Journal of Applied Physics

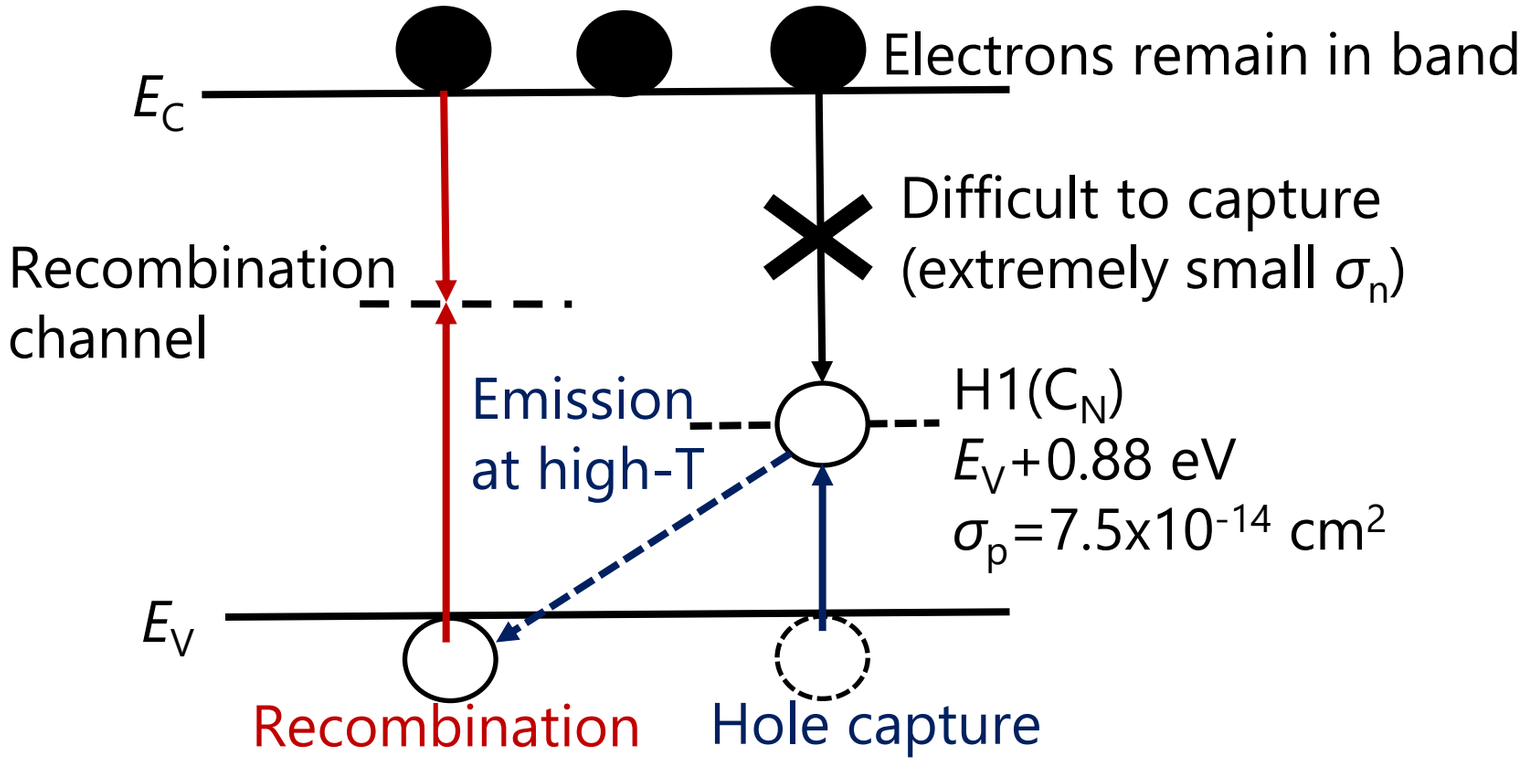

AIP Publishing

Journal of Applied Physics

ACCEPTED MANUSCRIPT

This is the author's peer reviewed, accepted manuscript. However, the online version of record will be different from this version once it has been copyedited and typeset.
PLEASE CITE THIS ARTICLE AS DOI: 10.1063/5.0041287

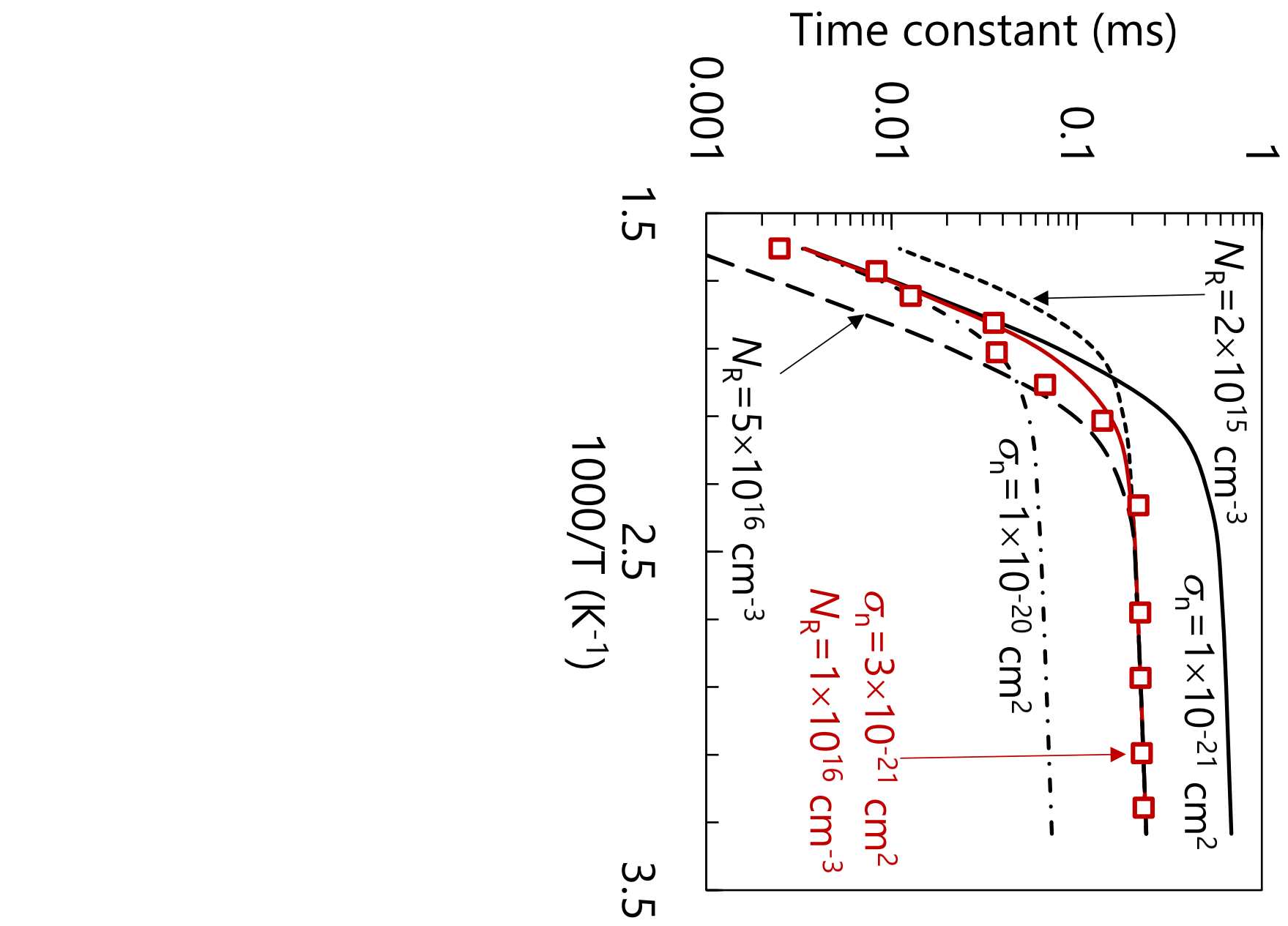

AIP Publishing

Journal of Applied Physics

ACCEPTED MANUSCRIPT

This is the author's peer reviewed, accepted manuscript. However, the online version of record will be different from this version once it has been copyedited and typeset.
PLEASE CITE THIS ARTICLE AS DOI: 10.1063/5.0041287

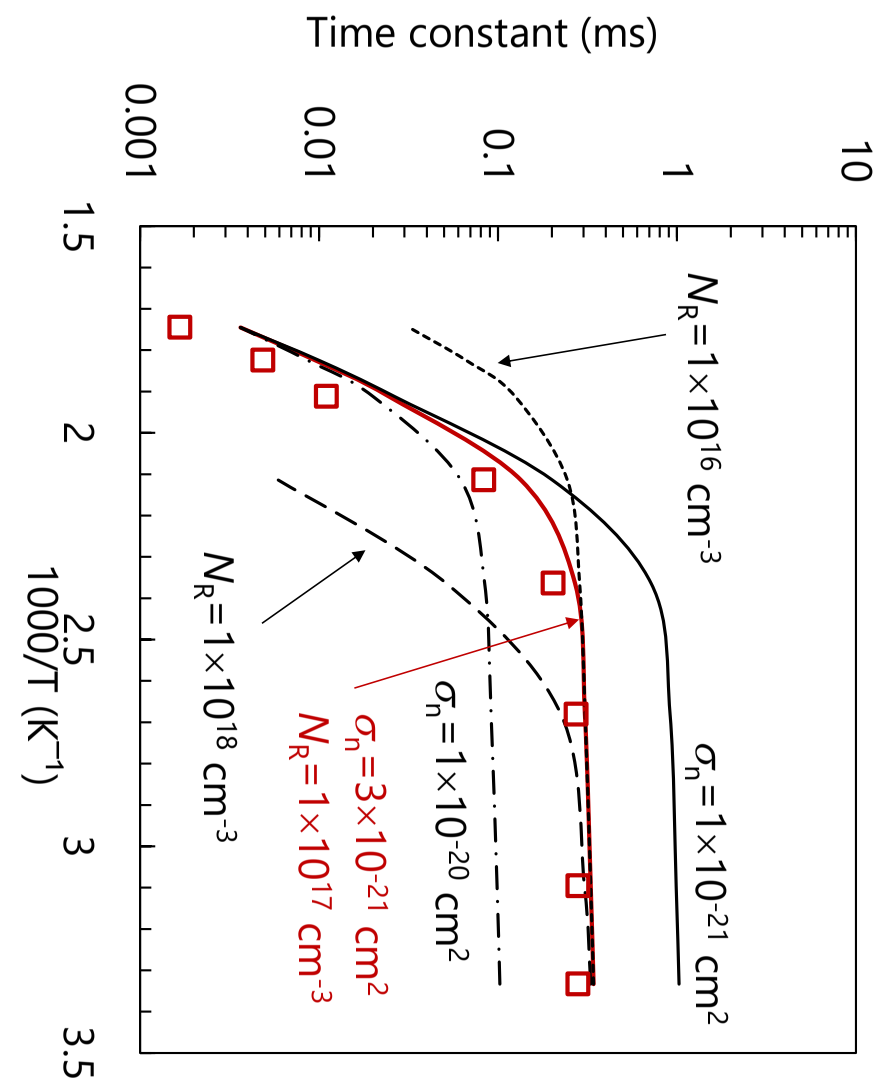

Journal of Applied Physics

PLEASE CITE THIS ARTICLE AS DOI: 10.1063/5.0041287